Chapter 6

Effect of changing pH and the Ionic Strength on the Surface Forces in Surfactant-Free Thin Aqueous Films

Abstract

This chapter describes the effect of pH-changes on the surface forces in thin, surfactant-free aqueous films containing a low background concentration of sodium chloride. Despite their exceedingly low surface elasticities, the surfactant-free aqueous films that have an equilibrium thickness about 100 nm are metastable for pH-values between 5 and 10. The extended DLVO theory was used to calculate hydrophobic force constant (K_{232}) from the measured equilibrium film thickness and estimated electrical surface potential. The results suggest that hydrophobic force in surfactant-free foam films is indifferent to pH changes.

6.1 Introduction

To gain an improved understanding of the molecular basis of hydrophobicity and hydrophobic attraction forces is fundamentally important and, additionally it is important for a wide range of applications in biological and colloidal systems. In the field of flotation, for instance, the long-range hydrophobic attraction force is supposed to play an active role in establishing the mineral-particle/air-bubble attachment needed to achieve selective ore enrichment.

For more than two decades, there have been on-going studies of the hydrophobic force in thin aqueous films between an air bubble and a hydrophobized solid surface (1-3), and between two hydrophobized solid surfaces (4-10).

Israelachvili and Pashley (4) established that in addition to the conventional DLVO (Derjaguin-Landau-Verwey-Overbeek) forces due to dispersion and electrostatic interactions, a long-range attractive interaction force operates between mica surfaces submerged in a cationic surfactant solution, particularly so near the surface charge neutralization concentration, and presumably arising because of the hydrocarbon-water contact.

The existence of a strong, *short-ranged* hydrophobic force has been convincingly verified, and its origin can readily be attributed to water restructuring occurring in the close vicinity of hydrophobic surfaces. However, the origin of the *long-ranged* hydrophobic force seems less clear. Different kinds of hydrophobic surface forces have been discussed and modeled, in particular: i) hydrogen-bond-propagated ordering of interfacial water molecules (4, 11); ii) bridging nano-bubbles of air between the hydrophobic surfaces (12). Moreover, a number of electrostatic interaction mechanisms have been subjected to critical tests, and likewise the notion of thin air films being present on hydrophobic surfaces submerged in water. Yet, none of these alternative approaches have been found justifiable for the most ideal hydrophobic surfaces that one can prepare for which the hydrophobic attraction is maximized.

Indeed, on the basis of the old, still probably rather incomplete notions of water structure, it is hard to justify a long-range hydrophobic attraction force. However, recent studies show that one may have to take into consideration the possible formation of clusters of water molecules inside thin water films (13, 14).

Sum Frequency Generation (SFG) studies (15, 16) indicate that the notion of hydrophobicity might be coupled with the appearance of dangling free hydroxyl bonds for about 25 percent of the surface water molecules. The SFG spectra of the interfacial water on silica surfaces coated with octadecyltrichlorosilane (OTS) are similar to those of ice, and include a prominent peak at 3,700 cm^{-1} due to the dangling (or free) OH groups oriented at the interface. This peak, which has been considered as a signature of hydrophobicity, has also been observed for the air/water and air/hexane interfaces. Thus, the SFG spectra obtained so far substantiate that an air bubble in water in effect acts as a hydrophobic substrate, and, hence, it is natural to raise the question whether there is also a long-ranged hydrophobic attraction between two air bubbles in water.

During the past decade, the thin film pressure balance (TFPB) technique has been used to study hydrophobic forces in single foam films (17-22). The studies have indicated

that a hydrophobic force is present in foam films formed at very low surfactant concentrations. This attractive force is of long-range, extending up to about 200 nm. It was also found that hydrophobic force in a foam film decreases with increasing surfactant concentration, implying that the strongest hydrophobic attraction is expected in the absence of any surfactant. Supposing that a strong hydrophobic force acts between two air bubbles in pure water would evidently make it a lot easier to understand why the rate of bubble coalescence is higher than anticipated on hydrodynamic grounds.

Extensive TFPB studies have been carried out of *surfactant-laden* foam films. On the other hand, little work has been done so far on *surfactant-free* thin films, in spite of their importance for the fundamental understanding of non-DLVO forces. Varying the pH may cause the ionic strength to change significantly, and possibly the water structure in the bulk and at the surface as well. Nevertheless, as far as possible one should try to isolate the effect of pH- changes on the surface forces operating in thin films. The major experimental obstacle encountered here is insufficient film stability for certain compositions of the film-forming aqueous solution. Aiming ultimately to investigate the origin of hydrophobic surface forces in thin films at low electrolyte concentrations, we present in the following an introductory study of the effect of changing pH on the surface forces in surfactant-free films.

6.2 Experimental section

A Nanopure water treatment unit was used to obtain deionized water (18.2 $M\Omega \cdot cm^{-1}$) after a two-stage distillation step. Sodium chloride (NaCl, 99.999%) from Sigma was used as the electrolyte. Sodium hydroxide (NaOH, 99.998%) from Sigma and hydrochloric acid (HCl, purum quality) from Fluka were used to adjust pH.

Equilibrium film thickness measurements were carried out in a Scheludko cell (23, 24). The inner radius of the film holder is 2.0 mm. Good wetting conditions were obtained by scratching the inner wall of the film holder with a sharpening stone, as suggested by Exerowa et al. (25). The cell was enclosed in a vapor-saturated chamber (to avoid evaporation that would shorten the life-time), which was water-jacketed to maintain the temperature at 24 ± 0.1°C. The chamber was placed on a tilt stage (M-044.00, Polytec PI), and careful adjustment for this tilt stage was needed to obtained horizontal foam films before each measurement. The whole device was mounted on an inverted microscope Olympus IX51. White light vertically reflected from the individual foam film is passed through a band-pass filter (LCS10-546, Laser components), then detected by a photosensor (H5784, Hamamastsu) with its power supply (C7169, Hamamastsu). The fluorescence condenser in the inverted microscope was specifically modified so that only a spherical regime (radius 0.045mm) of the film can be illuminated. The reflected light intensity was recorded by a PC-based data acquisition system. The film thickness was calculated using the micro-interferometric technique (23). During the experiments, the film radius was controlled in the range of 0.08-0.12 mm, where the change of the film radius has little effect on the equilibrium film thickness.

The pH of the electrolyte solutions were measured using a pH-meter with an accuracy of ±0.1 units. Generally, the contributions to the ionic strength, *I*, from ions other than mono-valent ones are negligible below pH about 10.0**,** as seen from the Bjerrum plot of the aqueous carbonate equilibrium diagram in a closed system. By

considering the charge neutralization condition, the ionic strength I is seen to be equal to $[Na^+]$ when pH > 5.7 (the "natural" pH). Below pH = 10, upon adding various amounts of NaOH to a 10^{-5} M NaCl solution**,** HCO_3^- predominates as the negative counterion. For pH < 5.7, realized by adding HCl, the ionic strength becomes equal to $[Na^+] + [H^+]$.

6.3 Experimental results

Preliminary TFPB experiments were conducted by one of the authors at the Max Planck Institute of Colloids and Interfaces at Golm, Germany. Horizontal thin films were formed using Scheludko cells with inner radii of 1.0 and 2.0 mm. Thin water films made from pure water are highly unstable; rupture occurs almost instantaneously. It is feasible, however, to produce metastable thin films at a low concentration of an inorganic electrolyte (*e.g.*, from 10^{-6} to $5x10^{-5}$ M NaCl) in the absence of any surfactant. When the NaCl concentration is increased further, the films become unstable. Figure 6.1 shows the lifetimes of films, formed using a Scheludko cell with an inner radius of 1.0 mm. As seen, the lifetimes decrease with increasing NaCl concentration from 10^{-6} to 0.1 M. The decrease in the film lifetime at high NaCl concentration is most likely related with the decrease in electrostatic disjoining pressure as a result of double-layer compression. Note that the data shown in Figure 6.1 were obtained at the Max Planck Institute of Colloids and Interfaces, where the solutions were prepared by using Millipore water, and NaCl was roasted at 600 °C for 5 h to remove surface-active contaminations (26). For the rest of the data shown in this paper, water was purified as described in the experimental section and *pro analysi* quality NaCl was used.

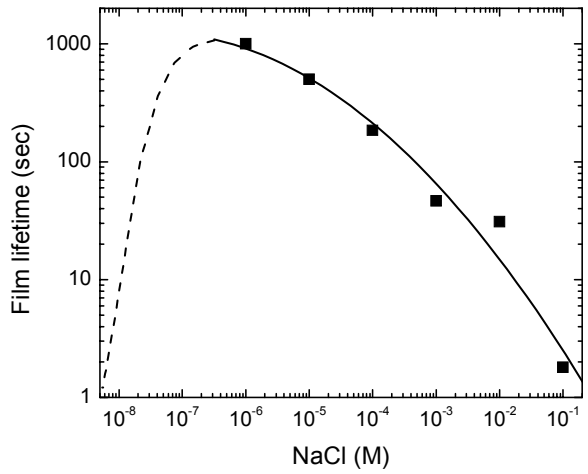

Figure 6.1 Effect of the NaCl concentration on the lifetime of thin films formed in a Scheludko cell with inner radius of 1.0 mm. The dotted line is hypothesized on the basis of the observation that the lifetime of a thin film formed from pure water is less than 1 second.

Figure 6.2 shows the equilibrium film thickness (H_e) of thin films in the presence of 10^{-5} M NaCl. H_e first increases with increasing pH, reaching a maximum at pH 6.2

prior to decreasing at higher pH-values. Supposedly, the relatively low H_e-values obtained at either low or high pH's are largely due to the higher ionic strength, which causes double layer compression. In the middle pH-range, the changes of H_e might be related to the changes of the surface potential as well. A detailed analysis is given below.

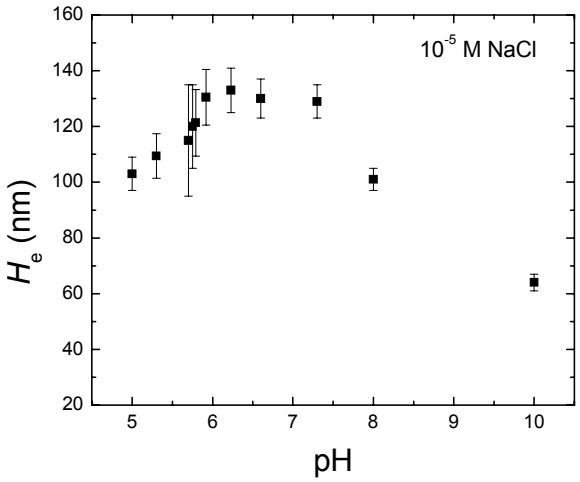

Figure 6.2 The influence of pH-changes on the equilibrium film thickness (H_e). Thin aqueous films were formed using a Scheludko cell with the radius 1.0 mm. The error bars show the maximal measuring errors.

6.4 Theoretical considerations

At equilibrium, H_e is determined by a balance between the overall disjoining pressure (Π) and the capillary pressure (P_c). Thus,

$$\Pi(H) - P_c = 0 \qquad [6.1]$$

where the capillary pressure, P_c, is given by

$$P_c = \frac{2\gamma}{r_c} \qquad [6.2]$$

γ denoting the surface tension of the film-forming solution, and r_c the radius of the cylindrical film holder, in which a spherically shaped meniscus is present. Since γ changes very little upon varying the pH from 5 to 10, the capillary pressure was considered to always remain the same and equal to 72.8 Pa.

According to the DLVO theory, the disjoining pressure in a foam film can be expressed as the sum of an electrostatic double-layer contribution (Π_{el}) and a van der Waals contribution (Π_{vw}):

$$\Pi = \Pi_{el} + \Pi_{vw} \qquad [6.3]$$

It has been shown, however, that the hydrophobic surface force may also play a role in foam films, particularly at low surfactant concentrations (18-21). To take this into account, Eq. [6.3] is rewritten by adding a third term on the r.h.s.:

$$\Pi = \Pi_{el} + \Pi_{vw} + \Pi_{hb} \qquad [6.4]$$

that includes a contribution of hydrophobic nature (Π_{hb}), which, for the case of a thin water film between *solid* hydrophobic surfaces, may be expressed as follows (11),

$$\Pi_{hb} = -\frac{bB}{2\pi}[\coth^2(bH/2) - 1] \qquad [6.5]$$

where H is film thickness, b^{-1} the decay length which, by comparison with experiments, Eriksson et al. found equal to 15.8 nm, and B is a constant representing the strength of the hydrophobic interaction.

For the comparatively thick films formed in our case, the van der Waals component is usually less than 1.0 Pa, and is therefore always negligible compared to the capillary pressure. On the other hand, the contribution of the hydrophobic force is presumably minimal at pH 6.2 where H_e is at its maximum value, i.e., 133 nm. Choosing the B-value derived by Eriksson, et al., (11), 0.6 mJ/m^2, and applying Eq. [6.5], the calculated hydrophobic force in a thin film of thickness 133 nm may amount to 5.3 Pa, which is also much less than the capillary pressure. Therefore, the major disjoining pressure component that counterbalances the capillary pressure at equilibrium should be the electrostatic double-layer repulsion. Nevertheless, the extended DLVO theory is applied here in order to study how hydrophobic force is affected by pH changes.

For the sake of consistence throughout this dissertation, hydrophobic force (Π_{hb}) is expressed by the following form (18):

$$\Pi_{hb} = -\frac{K_{232}}{6\pi H^3} \qquad [6.6]$$

where H is the distance between two charged surfaces and K_{232} is a hydrophobic force constant. An advantage of using Eq. [6.6] rather than Eq. [6.5] is that the former is of the same form as the van der Waals' pressure. Therefore, K_{232} can be directly compared with the Hamaker constant A_{232}. Substituting Π_{hb}=5.3 Pa and H=133 nm into Eq. [6.6] results in a K_{232} value of 2.4x10^{-19} J, which is in commensurate with the afore-mentioned values of B and b^{-1} in Eq. [6.5].

Substituting Eq. [6.4] into Eq. [6.1] with ignoring Π_{vw} leads to the following relationship:

$$\Pi_{el} + \Pi_{hb} = P_c \qquad [6.7]$$

Now, the equilibrium thickness, H_e, is for the most part more than twice the Debye length (κ^{-1}),

$$\kappa^{-1} = \left(\frac{\varepsilon_r \varepsilon_0 kT}{2e^2 N_A I}\right)^{1/2} \qquad [6.8]$$

where ε_0 and ε_r are the permittivity of the vacuum and the dielectric number of water, respectively, e the electronic charge, and N_A the Avogadro number. Hence, at least for the pH = 6.2 case, the double-layer repulsion (Π_{el}) may be accounted for by using the weak-overlap approximation. Now, Eq. [6.7] can be transformed into

$$64 c_s RT \Gamma_0^2 \exp(-\kappa H_e) - \frac{K_{232}}{6\pi H_e^3} = \frac{2\gamma}{r_c} \qquad [6.9]$$

where, as usual, $\Gamma_0 = \tanh(e\psi^0/4kT)$ and c_s denotes the overall electrolyte concentration in moles per m^3.

Inserting H_e = 133 nm and K_{232}= 2.4x10^{-19} J into Eq. [6.9] yields the surface potential ψ^0 at pH 6.2 (denoted as $\psi^0_{6.2}$): $\psi^0_{6.2}$ = - 46.4 mV. This value is significantly lower than the ζ- potential at pH 6.2 ($\zeta_{6.2}$ = -71 mV) measured by Li and Somasundaran (27), which is hardly surprising as there are a number of uncertainties in the connection between ψ^0 in Eq. [6.9] and the ζ- potential. In addition, the calculation of a ζ- potential from the measured electrophoretic mobilities involves several more assumptions (28). Nevertheless, we have assumed that the ζ- potential data due to Li and Somasundaran may reflect the *relative change* of the double-layer potential as a function of pH, and have therefore used the following relationship to estimate ψ^0 at pH-values different from 6.2:

$$\psi^0 = \frac{\psi^0_{6.2}}{\zeta_{6.2}} \zeta = 0.653\zeta \qquad [6.10]$$

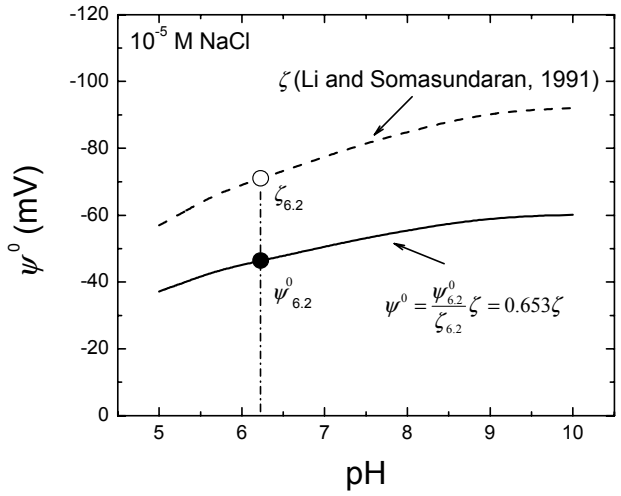

Figure 6.3 The estimated surface potential (ψ^0) shown as a function of pH. The filled circle represents the predicted surface potential (= - 44.6 mV) from the measured equilibrium film thickness at pH 6.2 (=133 nm) using Eq. [6.9]. The empty circle represents the measured ζ-potential (= -71.0 mV) at pH 6.2.

In Figure 6.3, our calculated ψ^0 values using Eq. [6.10] are represented by a solid line. For comparison, the measured ζ- potentials (27) are represented by a dashed line. It is worth noting that other investigators have reported ζ- potentials of significantly different magnitudes but showing much the same trend when plotted against the pH (29).

Next, we inserted the ψ^0 values shown in Figure 6.3 into Eq. [6.9] to calculate K_{232} values from the measured equilibrium thickness H_e, shown earlier in Figure 6.2. The results are shown in Figure 6.4. It is seen that all the K_{232} values are within the order of 10^{-19} J. As compared to the significant effects of surfactant concentration on hydrophobic force in foam films, presented in previous chapters, hydrophobic force in foam films appears to be indifferent to pH changes.

As is known, SFG technique may be used to characterize the hydrophobicity of air/water interface via the peak of free OH groups tangling toward the vapor phase. Based on ref (30), however, the peak of free OH bond does not noticeably increase until pH 13 and above, pointing out that the hydrophobicity of air/water interface hardly increases at pHs slightly above 5.7. Therefore, Figure 6.4 appears to lend support to the notion that hydrophobic force is related to the surface-induced water structure rearrangement.

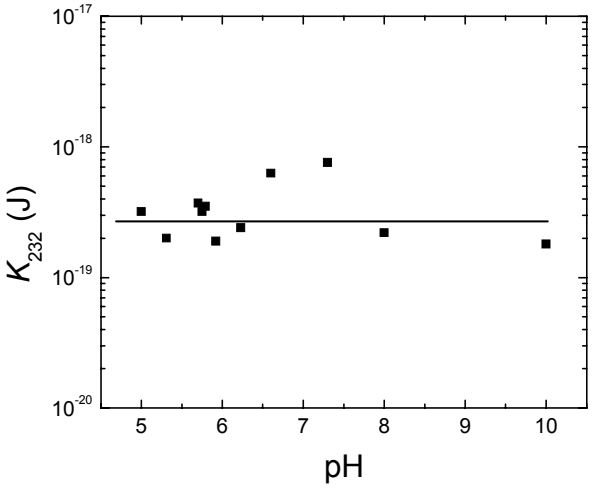

Figure 6.4 The estimated hydrophobic force constant (K_{232}) in Eq. [6.9] as a function of pH at 10^{-5} M NaCl.

Note that the present work only shows the relatively change of hydrophobic attraction as a function of pH changes. It is likely that either the electrical surface potentials estimated from zeta potentials deviate somehow from the real double-layer potentials, or *true* hydrophobic force was in the background of other stronger attractive forces of different origin. In addition, it is probable that the weak-overlap approximation for electrostatic double-layer force may not satisfactorily apply here. Figure 6.5 shows the area per charge, $a = e/\sigma$, on the film surfaces as a function of pH. The surface charge density σ was calculated from the ψ^0 values shown in Figure 6.3 using the following well-known relationship between the surface charge density and the surface potential resulting from the Gouy-Chapman theory:

$$\sigma = \sqrt{8RT\varepsilon_0\varepsilon_r c_s}\,\sinh\left(\frac{e\psi^0}{2kT}\right) \qquad [6.11]$$

It appears that surface area per (negative) surface charge has a maximum (= 440 nm^2) at the natural pH = 5.7. The circumstance that the *a*-values are smaller at higher as well as lower pH, is for the most part due to the increase in ionic strength as a result of adding HCl or NaOH. Note that these *a*-values are quite large.

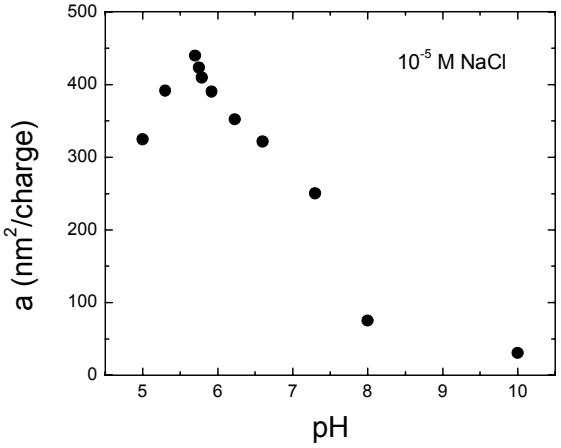

Figure 6.5 The area per (negative) surface charge plotted *vs.* pH**.**

6.5 Conclusions

In a closed (to prevent evaporation) surfactant-free system, it is feasible to form metastable thin films in the presence of a low concentration inorganic electrolyte using a Scheludko cell. The surfactant-free aqueous films studied in the present work have exceedingly low surface elasticities, estimated to be of the order 10^{-5} mN/m. Nevertheless, in the presence of 10^{-5} M NaCl the films are metastable in the pH-range 5-10 but unstable outside this range. This indicates that surface forces/film thickness are the dominant factors affecting the film stability. Similar conclusions were made in Chapter 4, which studies the kinetics of film thinning in the presence of 0.1 M NaCl and a nonionic surfactant at low concentration. The extended DLVO theory was used to estimate the contribution from hydrophobic force. There are no indications that the pH variable *per se* might have any significant impact on an alleged hydrophobic surface force within the separation range covered.

6.6 References

1. Blake, T. D.; Kitchener, J. A.; *J. Chem. Soc. Faraday Trans*. 68 (1979) 1435.

2. Yoon, R.-H.; Yordan, J. L. *J. Colloid Interface Sci*. 146 (1991) 565
3. Churaev, N.V., *Advances in Colloid and Interface Sci*. 114–115 (2005) 3.
4. Israelachvili, J. N.; Pashley, R. M., *Nature*, 300 (1982) 341.
5. Rabinovich, Ya, I.; Derjaguin, B. V., *Colloids Surf*., 30 (1988) 243.
6. Claesson, P.M., Christenson, H.K., *J.Phys. Chem*. 92 (1988) 1650.
7. Rabinovich, Y.I., Yoon, R.-H., *Langmuir* 10 (1994) 1903
8. Meyer, E. E.; Lin, Q.; Israelachvili, J. N., *Langmuir*, 21 (2005) 256.
9. Lin, Q.; Meyer, E. E.; Tadmor, M.; Israelachvili, J. N.; Kuhl, T. L., *Langmuir* 21 (2005) 251.
10. Zhang, J.; Yoon, R.-H.; Mao, M.; Ducker, W. A., *Langmuir*, 21 (2005) 5831.
11. Eriksson, J. C.; Ljunggren S. and Claesson, P.M., *J. Chem. Soc., Faraday Trans*. 2 85 (1989) 163.
12. Parker, J. L.; Claesson, P. M.; Attard, P.; *J. Phys. Chem*., 98 (1994) 8468.
13. Wernet, Ph.; Nordlund, D.; Bergmann, U.; Cavalleri, M.; Odelius, M.; Ogasawara, H.; Näslund, L. Å.; Hirsch, T. K.; Ojamäe, L.; Glatzel, P.; Pettersson, L. G. M.; Nilsson, A.; *Science* 304 (2004) 995
14. Chaplin, F.M., *Biophysical Chemistry* 83 (1999) 211.
15. Du, Q.; Superfine, R.; Freysz, E. and Shen, Y.R., *Phys. Rev. Lett*. 70 (1993) 2313.
16. Du, Q., Freysz, E. and Shen, Y.R., *Science* 264 (1994) 826.
17. Tchaliovska, S.; Manev, E.; Radoev, B.; Eriksson, J. C.; and Claesson, P. M., *J Colloid Interface Sci*. 168 (1994) 190.
18. Yoon, R.-H.; Aksoy, B.S., *J. Colloid Interface Sci*. 211 (1999) 1.
19. Angarska, J.K.; Dimitrova, B.S.; Danov, K.D.; Kralchevsky, P.A., Ananthapadmanbhan, K.P. and Lips, A., *Langmuir* 20 (2004) 1799.
20. Wang, L.; Yoon, R.-H., *Langmuir* 20 (2004) 11457.
21. Wang, L.; Yoon, R.-H., *Colloids Surfaces A: Physicochem. Eng. Aspects* 263 (2005) 267.
22. Wang, L.; Yoon, R.-H., *Colloids Surfaces A: Physicochem. Eng. Aspects*, in press.
23. Scheludko, A., *Adv. Colloid Interface Sci*. 1 (1967) 391.
24. Exerowa, D. and Kruglyakov, P. M., *Foam and Foam Films*, Elsevier, 1998.
25. Exerowa, D.; Zacharieva, M. Cohen, R.; Platikanov, D., *Colloid and Polymer Sci*. 257 (1979) 1089.
26. Muruganathan, R.M.; Krustev, R.; Ikeda, N.; Müller, H.J., *Langmuir*, 19 (2003) 3062.
27. Li, C. and Somasundaran, P., *J. Colloid and Interface Sci*., 146 (1991) 215

28. Lyklema, J.; Mysels, K.J., *J. Amer. Chem. Soc*. 87 (1965) 2539.

29. Yang, C.; Dabros, T.; Li, D.; Czarnecki, J.; Masliyah, J. H., *J. Colloid Interface Sci*. 243 (2001) 128.

30. Shen, Y.R., private communication (2004).